Performance of colloidal silica grout at elevated temperatures and pressures for cement fracture sealing at depth

Submitted to Journal of Petroleum Science & Engineering

SUBMISSION TO
JOURNAL OF PETROLEUM SCIENCE AND ENGINEERING

DATE:

TITLE:
Performance of colloidal silica grout at elevated temperatures and pressures for cement fracture sealing at depth

AUTHORS:
Arianna Gea Pagano*
Gráinne El Mountassir **
Rebecca Jane Lunn ***

POSITION AND AFFILIATION:
* PDRA, Department of Civil and Environmental Engineering, University of Strathclyde
** Senior Lecturer, Department of Civil and Environmental Engineering, University of Strathclyde
*** Professor, Department of Civil and Environmental Engineering, University of Strathclyde

CONTACT ADDRESS:
Dr Arianna Gea Pagano
Department of Civil and Environmental Engineering
University of Strathclyde
James Weir Building - Level 5
75 Montrose Street - Glasgow G1 1XJ, Scotland, UK
E-mail: arianna.pagano@strath.ac.uk

Submitted to Journal of Petroleum Science & Engineering

Performance of colloidal silica grout at elevated temperatures and pressures for cement fracture sealing at depth

Arianna Gea Pagano, Gráinne El Mountassir, and Rebecca J. Lunn

ABSTRACT

Hydrocarbon well decommissioning requires the long-term sealing of abandoned wells. Current plug and abandonment (P&A) operations are not always able to address all potential fluid migration pathways, resulting in the possible upwards migration of hydrocarbons from formations penetrated by the wellbore. The development of innovative materials to improve well sealing remains a major challenge .

This paper presents a proof of concept for the use of colloidal silica (CS)-based grout to improve the sealing performance of P&A operations. CS is a non-toxic suspension of silica nanoparticles (<100 nm) undergoing gelation upon destabilisation. Due to its excellent penetrability and controllable gel time, CS has the potential for repairing fine-aperture cracks within the cement sheath, at the cement/casing interface, or within a cement plug, where the penetration of cementitious grouts is restricted due to their relatively large particle size. In this study, the suitability of CS grout for deployment up to 1500 m depth was successfully demonstrated. Firstly, a range of CS grout mixes were investigated to test the feasibility of grout emplacement considering a timescale of 2 hr for pumping operations from the surface to depth. Secondly, to investigate the sealing performance, the CS grout was injected into fractured cement cores (0.2 and 0.5 mm fracture aperture) and exposed to pressure and temperature conditions simulating downhole scenarios up to 1500 m depth (based on gradients for North Sea, UK). Fracture permeability upon water injection was assessed pre- and post-

treatment. This work found that permeability values after treatment were reduced by three orders of magnitude, thus confirming the potential of CS grout for repairing fine-aperture cracks.

1. INTRODUCTION

Decommissioning of oil & gas production facilities is a topic of major interest, due to the on-going activity in the North Sea, UK and Gulf of Mexico, US. In 2020, the UK Oil and Gas Industry Association (OGUK) forecast the closure of more than 1600 hydrocarbon wells over the period 2020-2029, with overall associated costs of over £ 15 billion ((Oil & Gas UK, 2020)). Well decommissioning accounts for 49% of total decommissioning expenditure.

Plug and abandonment (P&A) operations represent a substantial component of well decommissioning. They are aimed at ensuring the long-term sealing of fluid migration pathways through abandoned wells to prevent the migration of hydrocarbon fluids between formations, and ultimately ensure the isolation of former producing zones and any penetrated formations from the surface or seabed ((Vrålstad, et al., 2019)). Furthermore, P&A operations should ensure appropriate sealing against the potential leakage of any other greenhouse gases to the surface, including biogenic methane (CH_4) from shallow sources (upper 1000 m below the seabed, (Böttner, et al., 2020)), as well as carbon dioxide (CO_2) stored within depleted oil reservoirs ((Nguyen, et al., 2020)). In all cases, long term wellbore integrity must be ensured. According to UK guidelines, two permanent cement barriers (primary and secondary barriers) in the wellbore are required to isolate each hydrocarbon-bearing zone with flow potential from the surface/sea bed. The primary barrier should be set in a suitable caprock above the zone with flow potential, and the secondary barrier should lie above this, again in a caprock layer and acts as a back-up to the primary barrier. The overall barrier comprises of the cement annuli and all cement plugs sealing the wellbore from rock to rock.

Many potential leakage pathways have been identified in wells with permanent cement barriers ((Gasda, et al., 2004), (Celia, et al., 2005), (Kiran, et al., 2017)). Normal operations during the well lifetime may cause the formation of micro-channels and micro-annuli within the cement sheath, as well as cracking and de-bonding at the casing/cement sheath interface. Rock porosity and fine

aperture fractures extending into the rock formation surrounding the well may also represent preferential flow paths. Fluid pathways may also exist through the well casing due to corrosion or shearing. Furthermore, leakages may occur through the cement plug itself due to the formation of internal cracks and/or degradation of the cement matrix, and at the cement/casing interface. The development of innovative materials to improve the sealing performance of P&A operations remains a major challenge with applications in hydrocarbon extraction wells, carbon dioxide storage, and geothermal.

This paper aims to provide a proof of concept for the use of colloidal silica based grout to provide long-term sealing of migration pathways encountered in wells. Colloidal silica (CS) is a non-toxic suspension of silica (SiO_2) nanoparticles (<100 nm) which may undergo gelation upon destabilisation, with the subsequent formation of siloxane bonds (Si – O – Si). Gelation is typically triggered by the addition of an electrolyte accelerator. Due to its low initial viscosity (similar to water), very small particle size and hence excellent penetrability, controllable gel time and low hydraulic conductivity ((Iler, 1979), (Yates, 1990), (Pedrotti, et al., 2017)), CS-based grout has found numerous applications in different fields over the past three decades. These include reservoir fluid-flow control systems within the petroleum industry ((Jurinak & Summers, 1991)), in situ containment of contaminated groundwater and soil ((Persoff, et al., 1995), (Moridis, et al., 1995), (Hakem, et al., 1997), (Moridis, et al., 1999), (Persoff, et al., 1999), (Manchester, et al., 2001)), soil stabilisation in tunnelling ((Bahadur, et al., 2007)) and for rock fracture sealing ((Butrón, et al., 2010)). Most of these studies have focused on the injection of colloidal silica into soil or porous or fractured rock.

For applications in the oil and gas sector, high pressure and high temperature conditions at depth may pose a limitation on the feasibility of CS grouting, potentially affecting its injectability, performance and durability. The effect of pressure on the stability of colloidal silica suspensions has been rarely reported ((Amiri, et al., 2011)), and does not seem to be significant. On the other hand,

the effect of temperature on gel time and gel microstructure has been widely investigated ((Hunt, et al., 2013), (Amiri, et al., 2011), (Butrón, et al., 2009)). In all studies, temperature is shown to decrease the gel time due to an increased rate of collision between silica nanoparticles. Therefore, the feasibility of pumping CS to significant depths will be limited by the temperature increase, due to the geothermal gradient, which may result in premature gelling of the grout within the wellbore. Further, the formation of a looser gel network due to the increased gelation kinetics ((Amiri, et al., 2011)) might affect the sealing performance of CS gel at high temperatures. Thus, experimental evidence is needed to assess the suitability of CS grout for deployment in downhole conditions.

To this end, an experimental investigation on the application of CS grout, at relevant downhole conditions up to 1500 m depth (based on North Sea gradients), was carried out in this study. First, the effect of temperature on the gel time of CS grout prepared at different electrolyte concentrations was investigated in order to assess the injectability of the grout at depth. Then, cement cores with constant fracture apertures were created and treated with CS grout at selected temperature and pressure combinations (from 20 to 80 °C, and from 0 to 15 MPa respectively), simulating downhole conditions at depths up to ~1500 m. The effectiveness of the treatment in terms of permeability reduction was investigated by performing flow-through core experiments before and after treatment. The effect of two different values of fracture aperture (0.2 and 0.5 mm) on the permeability reduction was also considered. Microstructural changes after treatment were monitored by means of X-ray Computer Tomography (X-CT) to support the results of the flow-through core experiments.

2. MATERIALS AND METHODS

2.1. Colloidal silica grout

In this study, MasterRoc® MP320 Part A was used as the colloidal silica suspension (viscosity at 20 °C: ~10 mPa·s, density at 20 °C: 1.3 kg/l, silica concentration by mass: 40 %, pH: 9.5 to 9.8). An accelerator (MP320 Part B) is also provided by the manufacturer to induce gelation. According to the manufacturer's recommendations, the gel time of the grout (Part A + Part B) may be adjusted between 6 minutes and 700 minutes by varying the quantity of Part B added to Part A (B:A ratio by volume of 30 % and 10 % respectively, for grout mixes prepared at 8 °C). Only MP320 Part A was used in this study, whereas different NaCl accelerators at varying molarities were prepared in the laboratory to induce grout gelation.

For viscosity and gel time measurements at temperature up to 85 °C, six CS grout samples were prepared. All grouts were prepared at 20 °C, prior to exposure to higher temperature. One of the six grout samples was prepared by mixing the as-delivered CS suspension with de-ionised water at a CS:water ratio of 5:1 by volume. The remaining five grouts were prepared by mixing the CS suspension with an electrolyte accelerator at a 5:1 CS:accelerator ratio by volume. NaCl was adopted as the electrolyte accelerator at varying molarities (i.e. moles of NaCl per litre) (0.4 M, 0.5 M, 0.6 M, 0.7 M, and 1.0 M). All grout samples had a pH between 7.7 and 7.8 after mixing.

For flow-through core experiments, CS grout was prepared by mixing the as-delivered CS suspension with de-ionised water at a CS:water ratio of 5:1 by volume. Unlike conventional CS based grouts, no electrolyte accelerator was added to induce gelation in the flow-through core experiments. This was to determine whether the presence of cations released by the cement into the pore fluid would be sufficient to induce grout gelation, despite the absence of an electrolyte accelerator within the grout mix.

2.2. Viscosity measurements of CS grout at high temperature

Viscosity measurements on CS grout samples were carried out to assess the effect of temperature on the gel time, both with and without the addition of an electrolyte accelerator to the grout mix. The purpose of these experiments was to identify a range of grout mixes exhibiting low viscosity (< 10 mPa·s) for up to 2 hours after mixing and exposure to increasing temperature from 20 °C to 85 °C, thus ensuring the feasibility of grout transportation and injection to 1600 m depth (assumed pumping times of 30-45 mins per km, plus 1-hour injection, based on discussion with industry partners).Viscosity measurements were performed with a Cole-Parmer Rotational Viscometer, using a standard L-series spindle (L1). During each test, the number of revolutions per minute (rpm) was ranged from 100 to 0.3, corresponding to a measureable viscosity range of ~9 - 20000 mPa·s. Each beaker containing a grout sample was placed in a water bath and exposed to a gradually increasing temperature, 'ramping up' from 20 °C to 85 °C in 2 hours to simulate grout transportation to ~1600 m and injection. After ramping, temperature was then kept constant. Grout evaporation, during temperature ramping and stabilisation, was prevented by means of a latex membrane. The evolution of viscosity against temperature was continuously monitored over time.

2.3. Cement cores

The cement cores tested in this study were prepared by mixing ordinary Portland cement (CEM II/A-L, class 42.5N) with de-ionised water at a water:cement ratio of 0.375 by mass. Cement paste was prepared in a rotary mixer according to BS EN 196-1:2005 and cast into bespoke silicon rubber moulds. Two-piece moulds were used to cast six cylindrical cores (S1 to S6) with diameter 37 mm

and height 75 mm. After 24 hours, the hardened cement pastes were demoulded and cured in de-ionised water for (at least) 27 days under controlled temperature conditions (20±1 °C).

A schematic view of the geometry of the cores tested in this study is shown in Figure 1. Cores were designed to consist of two halves: a flat half, and one containing a 25 mm wide, 75 mm long fracture with theoretical mechanical apertures, $\boldsymbol{b}$, of 0.2 mm (set 1, cores S1, S2, S3) or 0.5 mm (set 2, cores S4, S5, S6). Actual mechanical apertures were expected to be smaller than their theoretical value due to inaccuracies of the designed moulds. This was confirmed by microstructural analyses carried out on cores S1 and S4 prior to treatment, showing average mechanical apertures of 0.12 mm and 0.35 mm respectively (Table 1). Detailed information about the microstructural analysis procedure is reported in Section 3.3.

Core	Designed mechanical aperture [mm]	Mechanical aperture from X-CT data [mm]	Temperature during treatment with CS [°C]	Pressure during treatment with CS [MPa]	Simulated condition
S1	0.2	0.12	20	0	Ambient
S2	0.2	-	60	11	1.1 km depth
S3	0.2	-	80	15	1.5 km depth
S4	0.5	0.35	20	0	Ambient
S5	0.5	-	60	11	1.1 km depth
S6	0.5	-	80	15	1.5 km depth

Table 1. Fracture apertures prior to treatment and temperature and pressure conditions during treatment with CS of the cores tested in this study. Pressure and temperature combinations for core S2, S3, S5 and S6 were selected by assuming a hydrostatic pressure gradient, and a temperature gradient of ~1.5 °C per 100 ft and North Sea temperature of 5 °C.

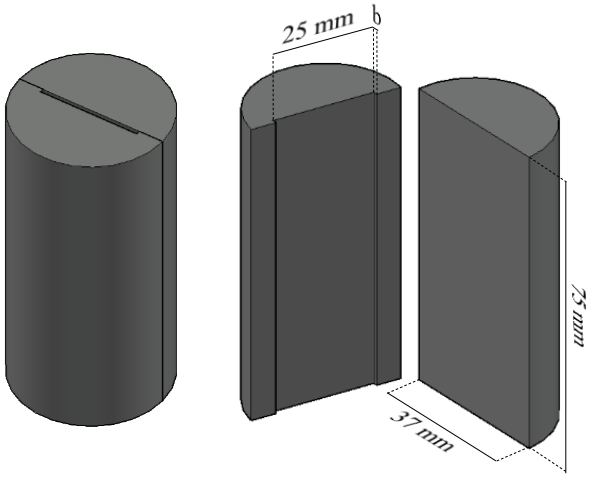

Figure 1. Designed core geometries.

2.4. Flow-through core experimental procedure

Treatment with CS grout and permeability measurements pre- and post-treatment, carried out to assess the sealing performance of the grout, were performed by means of a bespoke high pressure/high temperature Hassler-type core holder (Figure 2). A confining pressure around the core of 3.5 MPa was applied, to prevent water bypass around the core, and kept constant throughout using a manual hydraulic pump. Fluids for treatment (CS grout) and permeability measurement (tap water) were injected into the cores with a Cole-Parmer HPLC dual piston pump. High temperature was applied to the core via an external silicon heater mat connected to a 240V heater control box, and insulated using a lagging jacket.

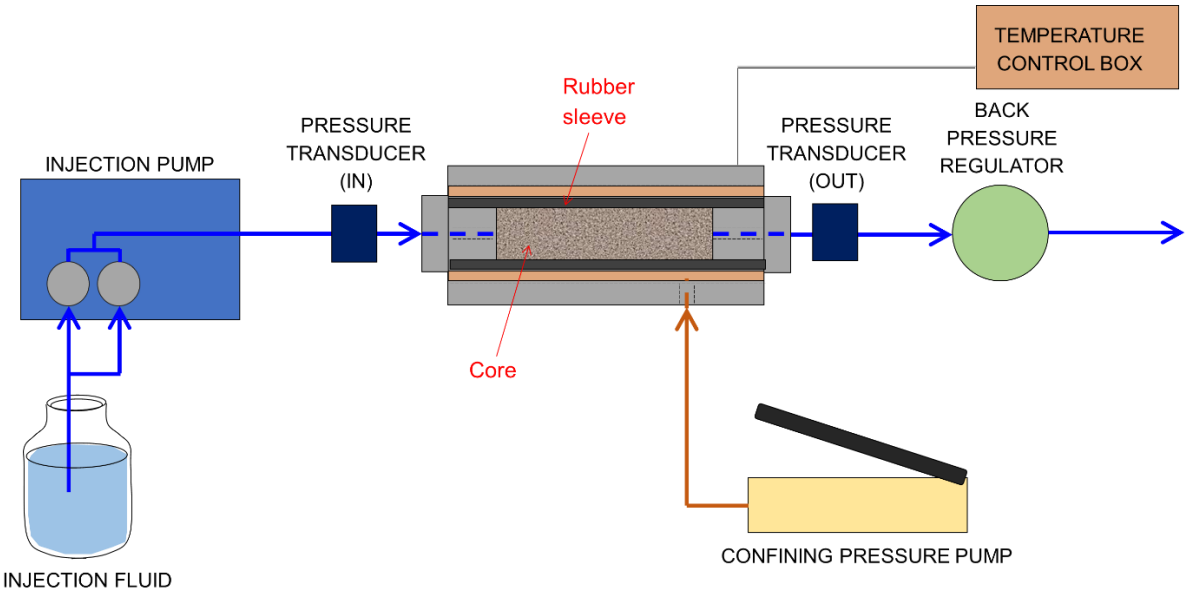

Figure 2. Schematic view of the high pressure and high temperature Hassler core holder.

Flow-through core experiments were performed as follows:

Stage 1 – Pre-treatment hydraulic characterisation. The hydraulic properties of each fractured core were determined prior to treatment with CS. The outlet core pressure was fixed at atmospheric pressure. Laboratory tap water was then injected into the core in consecutive injection steps, with increasing flow rates of 0.79, 3.94, 7.91 and 11.89 ml/min, and the corresponding rise in the inlet pressure was continuously monitored. An example of selected flow rate values and recorded inlet and outlet pressure prior to treatment are reported in Figure 3 for core S1.

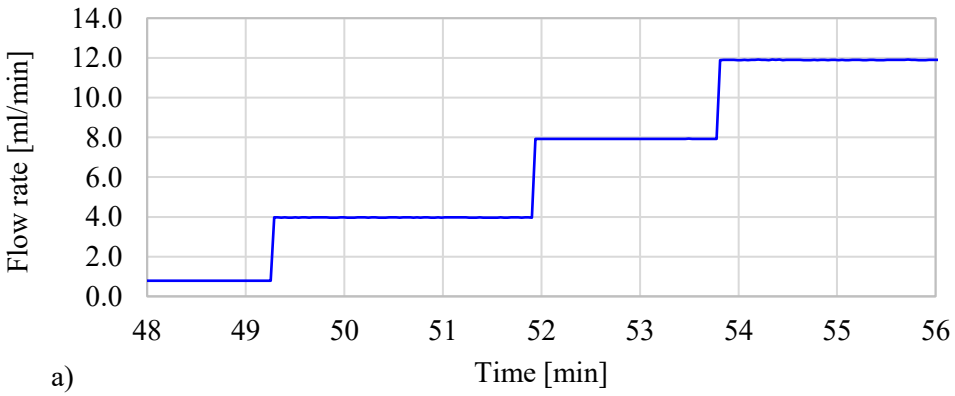

a)

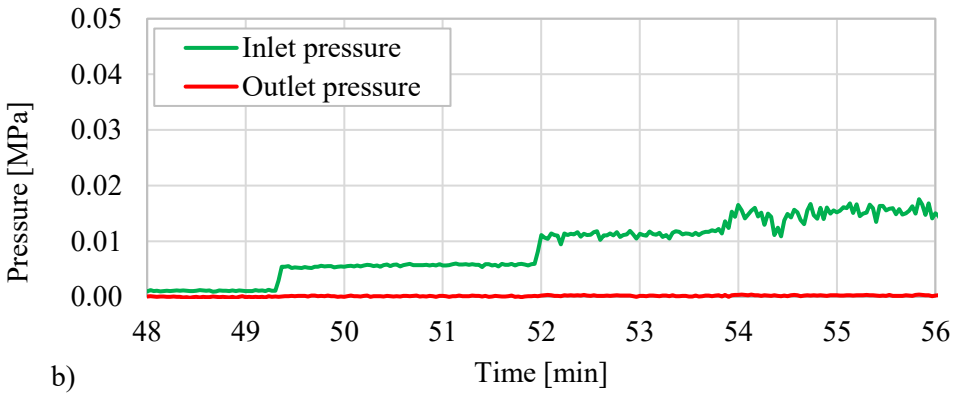

Figure 3. Example of selected flow rates (a) and resulting inlet and outlet pressure (b) during pre-treatment hydraulic characterisation (core S1).

Stage 2 – Pre-treatment microstructural analysis (core S1 and S4 only). X-ray tomographies of selected cement cores were carried out with a Nikon XTH320 micro-CT scanner to characterise the exact fracture geometry, and any other relevant microstructural feature, prior to treatment. Scans were performed at 138 kV energy and 80 µA current, with a voxel size of 50x50x50 µm. Each core was placed into a sealed rubber mould during the scan to prevent water evaporation from the cement matrix.

Stage 3 – Treatment with CS grout (CS grout injection and exposure to environmental conditions). Before treatment, each core was pre-conditioned overnight in the core holder by saturating the fracture with tap water. Then, treatment was performed by injecting CS grout into the core at a constant flow rate (0.79 ml/min), until CS grout was seen at the outlet sampling port. Following CS injection, the cores were left within the core holder for 10 hours, at one of the three selected pressure and temperature combinations, as shown in Table 1. These pressure and temperature combinations were selected by assuming a hydrostatic pressure gradient, and a temperature gradient of ~1.5 °C per 100 ft (30.48m) and North Sea temperature of 5 °C. The cores were then left to equilibrate with ambient conditions for a further 62 hours.

Stage 4 – Post-treatment microstructural analysis (core S1 and S4 only). Selected cores were imaged again after treatment to determine the spatial location of CS grout within the fracture, and to identify any other microstructural change. The same settings as in Stage 2 were used for the post-treatment scans.

Stage 5 – Post-treatment hydraulic characterisation. Hydraulic properties were characterised after treatment on each core by injecting tap water. While keeping a constant confining pressure of 3.5 MPa, the inlet (injection) pressure was ramped up to a target pressure of 1.45 MPa in consecutive 0.2-MPa steps, over ~ 3.5 hours. The target pressure was then kept constant for up to 9 hours (Figure 4). The flow rate corresponding to each inlet pressure was continuously monitored to characterise the fracture's hydraulic properties after treatment.

The hydraulic characterisation was performed using tap water only as the injection fluid, and by considering the resistance of the grout to pressure differentials. Note that the influence of potential degradation of the grout due to possible chemical interactions with downhole fluids was considered to be outside the scope of this study.

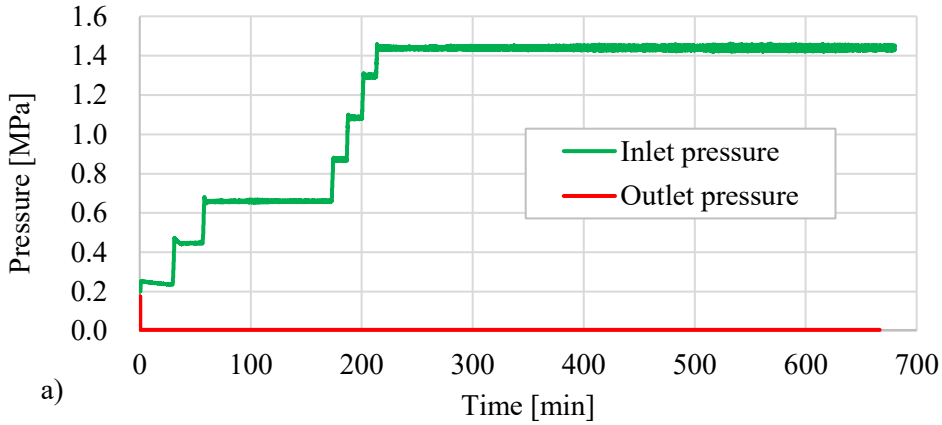

a)

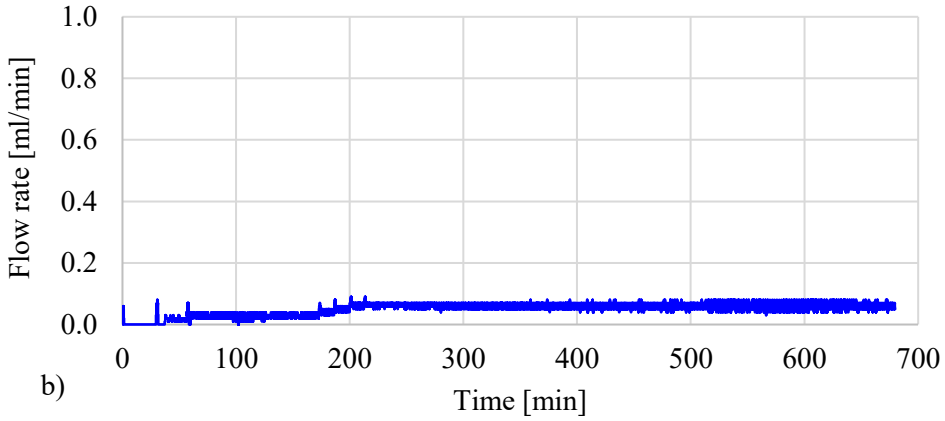

Figure 4. Example of selected inlet and outlet pressure (a) and resulting flow rates (b) during post-treatment hydraulic characterisation (core S6).

2.5. Evaluation of hydraulic aperture and permeability changes

Assuming laminar single-phase flow, the theoretical volumetric flow rate Q through a smooth parallel fracture, such as that created within the cement cores, of width w and length L is given by the Boussinesq equation ((Witherspoon, et al., 1980)):

$$Q = \frac{wb^3}{12\mu}\frac{\Delta P}{L} \quad (1)$$

where μ is the fluid viscosity, ΔP is the pressure differential across the fracture, and b is the mechanical aperture, taken as the vertical distance between the two fracture walls. Where the hypothesis of smooth fracture walls does not hold, the mechanical aperture in Equation 1 is replaced by the hydraulic aperture, b_h, taking into account the effect of roughness and geometrical irregularities on the fluid flow. The hydraulic aperture is in turn related to the fracture permeability K, as follows:

$$K = \frac{b_h^2}{12} \quad (2)$$

The experimental data on volumetric flow rate and differential pressure collected during the flow-through core experiments were used to derive the hydraulic aperture and the fracture permeability from Equation 1 (solved for $b = b_h$) and Equation 2 respectively. In all calculations, water flow was assumed to occur only through the 25 mm wide fracture (w=25 mm in Equation 1), i.e. the permeability of the cement matrix was assumed to be negligible with respect to the permeability of the fracture. In addition, water flow at the interface between the two core halves, to the left and right sides of the fracture, was assumed to be zero.

2.6. Microstructural analysis

Microstructural changes in fracture geometries were analysed using X-ray CT carried out on selected cores. Nikon software CT Pro 3D was used for the 3D reconstruction of the image sequences and the beam hardening correction was applied to minimise edge effects. Image processing was carried out using the Avizo 9.3 software. The X-CT data within half a cm from the inlet and the outlet of the cores were discarded before image processing was carried out, in order to remove image artefacts. In addition, a median filter was applied to all image sequences prior to segmentation in order to reduce noise. Different phases within the cores - namely cement matrix, colloidal silica grout (if present), water and air - were identified using the multiphase watershed segmentation tool implemented in Avizo.

3. RESULTS AND DISCUSSION

3.1. Evaluation of CS grout suitability at high temperature

Figure 5a shows the viscosity evolution of CS grouts, prepared at different accelerator concentrations, and exposed to a ramping temperature, as described in Section 2.2. The evolution of temperature with time, for all experiments, is plotted in Figure 5b.

An initial grout viscosity at room temperature (20±1 °C) of < 9 mPa·s was measured for all samples. The subsequent increase in viscosity, indicates the onset of the gelation process. Gel time was inferred from Figure 5a as the intersection between the linear regression of all the points at viscosity higher than 2000 mPa·s and the x-axis (Bergna and Roberts, 2005).

In the absence of a NaCl accelerator (DI water, Figure 5a), the silica suspension did not form a gel, even after 12 hours of exposure to 85 °C. This result suggests that CS grout prepared with no electrolyte accelerator would definitely be pumpable to depths of ~1600 m (corresponding to ~85 °C) as the initial low viscosity of the grout can be maintained at elevated temperature over a significant period of time.

In the presence of NaCl, the gel time was observed to vary with accelerator concentration in a non-linear fashion, with faster gelation occurring with increasing accelerator concentration (Figure 5a). For comparison, predicted gel times at room temperature for the same grout compositions are also reported in Table 2. These were obtained by using the analytical model proposed by Pedrotti et. al (2017) for the same colloidal silica suspension (MP320 Part A). As expected, ramping up the grout temperature significantly sped up the gelation process. At NaCl concentrations of 0.4 M, 0.5 M and 0.6 M, gelling occurred after reaching the target temperature of 85 °C at times of 9.6, 3.5 and 2.2 hours respectively. These results suggest that NaCl concentrations of between 0.4 M and 0.6 M would be pumpable to depths of 1600 m, if a pumping period of ~2 hours is considered. At higher NaCl

concentrations (0.7 M and 1.0 M), gelling occurred before reaching the target temperature (at ~70 °C and ~80 °C, 1.8 and 1.1 hours respectively, Figure 5 a and b) and hence would not be pumpable to depths higher than 1.25 and 1.5 km respectively.

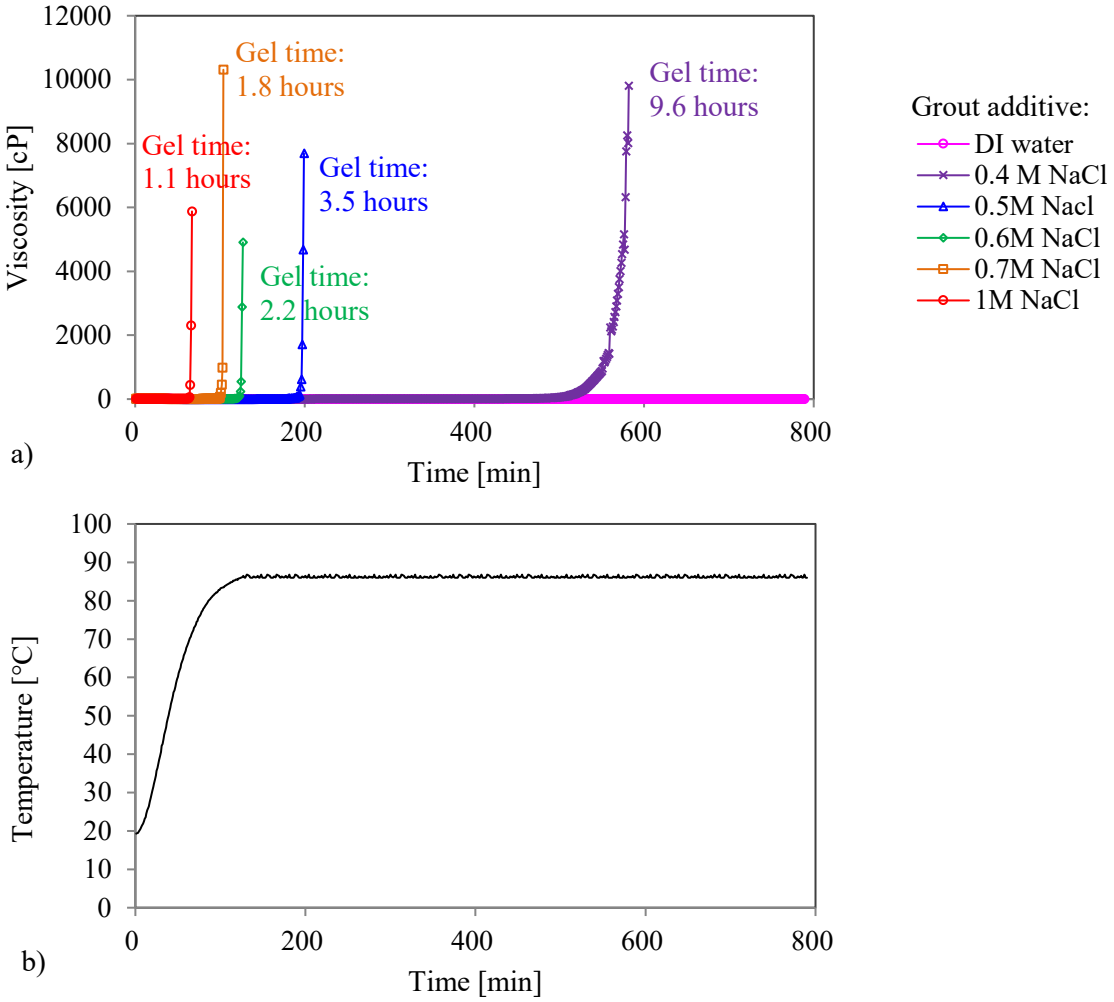

Figure 5. (a)Viscosity evolution overtime of CS grout samples at different electrolyte concentrations, exposed to ramping temperature, and (b) temperature evolution overtime during viscosity measurements

NaCl concentration [M]	Gel time [min]	
	Pedtrotti et al. 2017 (20°C)	**Current work (ramping temperature, 20°C to 85°C)**
0.4	4447	576
0.5	3114	208
0.6	2181	132
0.7	1528	108
1	528	68

Table 2. Comparison between gel time predictions from Pedrotti et al. (2017) and current work. Predicted gel times at room temperature were obtained by assuming a pH of 7.77 and a particle diameter of 15 nm.

3.2. Hydraulic aperture and fracture permeability

Figure 6a shows the evolution of fracture permeability against hydraulic aperture before and after treatment with CS grout. As expected, hydraulic apertures prior to treatment are lower than mechanical apertures, with an average hydraulic aperture value of 0.06 mm for set 1 (designed mechanical aperture of 0.2 mm, cores S1, S2 and S3) and 0.15 mm for set 2 (designed mechanical aperture of 0.5 mm, cores S4, S5, S6). This resulted in fracture permeability values for each set of order 10^{-10} m^2 and 10^{-9} m^2 respectively, prior to treatment.

It should be noted here that even though no electrolyte accelerator was mixed with the CS grout in these tests, the hydraulic aperture and, hence, fracture permeability was significantly reduced after treatment in all cores. Hydraulic apertures after treatment were all observed to lie within a range of 1 - 5 μm. These reductions correspond to decreases in the fracture permeability of approximately 3 orders of magnitude in all cases, with the grouted fracture permeability of order 10^{-13} m^2 for set 1 and 10^{-12} m^2 for set 2.

The results of the flow-through core experiments show a negligible effect of pressure and temperature conditions on the effectiveness of the treatment in terms of permeability reduction. This is shown in Figure 6b, where fracture permeability values after treatment at different pressure

conditions are plotted against temperature. Here, post-treatment permeability values for each set of cores seem to be almost constant, irrespective of the pressure and temperature conditions. These results suggest that reservoir conditions up to 1.5 km in depth would not affect the performance of CS grout in terms of sealing leakage pathways.

It is interesting to compare the values of fracture permeability obtained after grouting to the hydraulic properties of pure colloidal silica gel. Moridis et al (1996a) and Wong et al (2018) reported hydraulic conductivity values of colloidal silica samples after gelling in the order of 10^{-9} – 10^{-8} m/s, corresponding to permeability values of 10^{-13} – 10^{-12} m^2 if water at 20 °C is considered as the permeating fluid. Given that all cores achieved final permeability values within this range, it is reasonable to assume that, after treatment, the water flow induced by the pressure differential across the fracture is now controlled by the connected porosity of a newly formed gel matrix running homogeneously throughout the fracture. This is despite the absence of an electrolyte accelerator in the grout mix. Based on the lack of gelling observed in the earlier viscosity test at high temperature for CS grout prepared only with DI water (Figure 5), here gelling and the formation of siloxane bonds has most likely been triggered by the presence of cations (predominantly calcium ions, Ca^{2+}) on the cement fracture surfaces that have been released by the cement into the pore fluid present within the cement matrix and fracture. This suggests that CS grout prepared with no electrolyte accelerator may still successfully destabilise and gel, and hence significantly reduce the fracture permeability, when in contact with available calcium cations deriving from cement hydration. It remains to be investigated whether the addition of an electrolyte accelerator to the grout mix would be required for aged cements, where the availability of calcium cations may be more limited. If sufficient cations are not available, electrolyte concentration could be carefully tailored to ensure pumpability to target depths, as shown in Section 3.1.

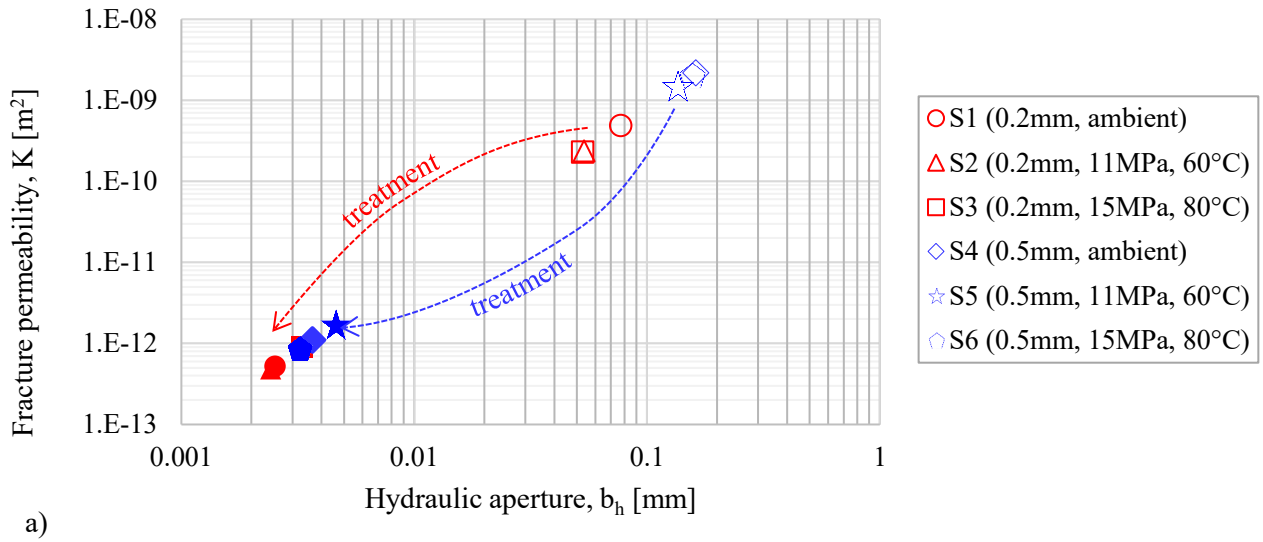

a)

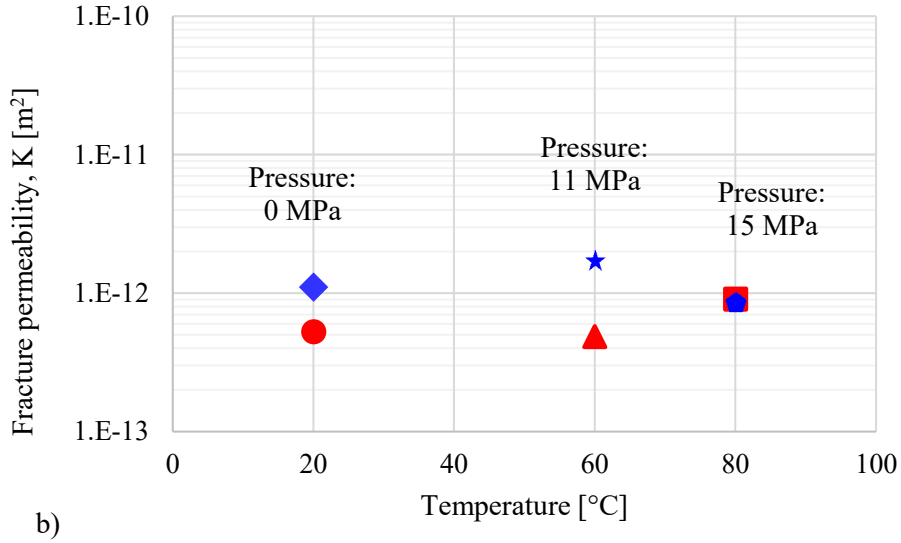

b)

Figure 6. Evolution of fracture permeability as a function of (a) hydraulic aperture, and (b) temperature. Open symbols (○△□◇☆⬠) denote untreated cores; filled symbols (●▲■◆★⬟) denote treated cores. Designed mechanical fracture apertures of 0.2mm are denoted in red; and 0.5mm are denoted in blue.

3.3. Microstructural analysis before and after treatment

Microstructural changes in fracture geometries were analysed using X-ray CT carried out on two cores, namely S1 and S4, before and after treatment with colloidal silica.

The volume rendering of the four segmented phases, namely cement matrix, water, air and colloidal silica grout before and after treatment for cores S1 and S4 are shown in Figure 7a and 7b respectively. In both cores, the fracture space is shown to be entirely filled by a combination of water and air prior to treatment. Initial average fracture apertures, previously reported in Table 1, were quantified from the volumes occupied by the water and air, by assuming a fracture width and length of 25 mm and 65 mm respectively (i.e. width and length of the imaged core). As mentioned in Section 2.3, the average mechanical fracture apertures derived from the X-CT data (0.12 mm for S1, 0. 35 mm for S4) are consistently smaller than the designed mechanical fracture apertures (0.2 mm and 0.5 mm).

After treatment with colloidal silica, the fracture space in both cores is occupied by a continuous CS grout phase, which is present throughout, from inlet to outlet (shown in red in Figure 7). Water and air phases are still present within the fracture but appear to be discontinuous at the resolution and voxel size of the X-ray tomographies. The X-CT data support the hypothesis that post-treatment flow properties are well described by the permeability of a continuous CS gel matrix filling the fracture and that no open channels remain that connect the inlet to the outlet.

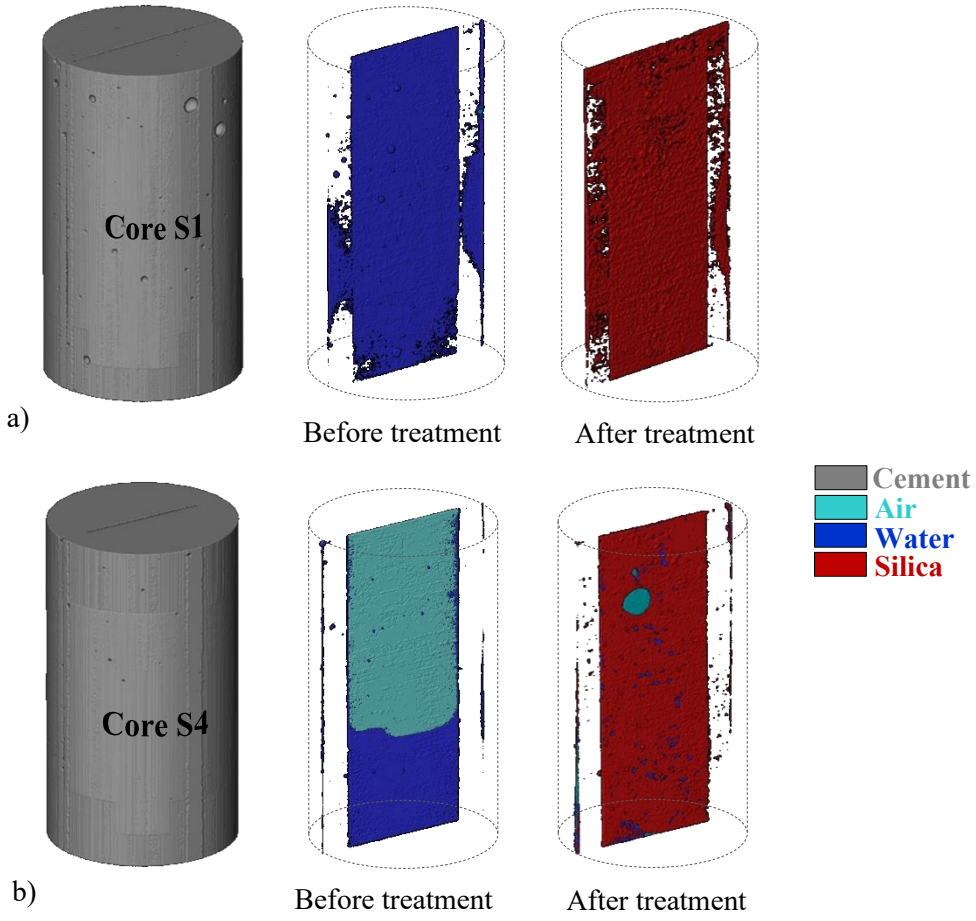

Figure 7. 3D volume rendering of 4 phases detected from x-ray tomographies – cement, air, water and silica –before and after treatment with colloidal silica for (a) core S1, and (b) core S4.

3.4. Grout fracturing and self-healing

The permeability values presented in Section 3.2 were derived for all cores from the average pressure differential across the fracture and measured flow rate values after stabilisation at each pressure step during pressure ramping. Cores S2, S3, S4 and S6 were able to withstand a pressure differential ramped up to 1.45 MPa for ~12 hours, after which the permeability test was stopped. On the other hand, cores S1 and S5 exhibited a sudden drop in the pressure differential and flow rate increase about 45-50 minutes after reaching the target pressure of 1.45 MPa, indicating a permeability increase. This suggested that a pressure differential of 1.45 MPa in these cases induced fracturing of the silica gel, possibly creating one or multiple open channels connecting the inlet to the outlet.

The permeability values before treatment, after treatment and at water breakthrough are reported in Figure 8 for cores S1 and S5. Although the fracture permeability of both cores increased significantly at the moment of the water breakthrough (~$1.4 \cdot 10^{-11}$ m^2 for core S1, ~$7.6 \cdot 10^{-11}$ m^2 for core S5), it was still observed to be at least one order of magnitude lower than the fracture permeability before treatment (~$4.9 \cdot 10^{-10}$ m^2 for core S1, ~$1.5 \cdot 10^{-9}$ m^2 for core S5).

To gain a better insight into the water breakthrough mechanism inducing the observed permeability increase, core S1 was imaged again after breakthrough, as shown in Figure 9. Despite the significant permeability increase, only an isolated crack towards the core's inlet was detected with the X-ray tomography; a clear channel connecting inlet to outlet was *not* visible. This was assumed to be due either to the formation of fissures/channels smaller than the resolution of the X-CT, or to the deformable nature of the gelled grout. In the latter case, it is possible that even after breakthrough, the gelled grout filling the fracture was able to 'self-heal' once the pressure differential (and, hence, water flow) across the core was removed.

In order to test this hypothesis, cores S1 and S5, which were submerged with tap water for storage during the covid pandemic (a duration of 5 months after the previous test) were tested again under the same conditions as for the post-treatment permeability tests. Both cores were able to withstand a pressure differential of up to 1.45 MPa, and no water breakthrough was observed for the entire duration of the tests (~12 hours). The permeability derived from these tests are also reported in Figure 8. The 'self-healed' permeability values of both cores were observed to be comparable to, or even lower than, those exhibited before water breakthrough (from ~$5.3 \cdot 10^{-13}$ m^2 to ~$5.4 \cdot 10^{-13}$ m^2 for core S1, from ~$1.8 \cdot 10^{-12}$ m^2 to ~$7.5 \cdot 10^{-14}$ m^2 for core S5), thus proving the ability of the gelled grout to self-heal in the absence of a continuous flow through the fracture. This suggests that, even if pressure differentials become high enough to fracture the grout after treatment, the grout could still regain integrity against future leakages if conditions suitable for self-healing occur. In addition, if there are

concerns over the possibility of continuous high pressure differentials downhole that might cause gel fracturing, further CS grout treatments might be considered after first gelling (prior to final abandonment) to increase the sealing capacity of the grout and avoid breakthrough, thus improving the grout's durability. Further laboratory and field testing would be required to investigate this.

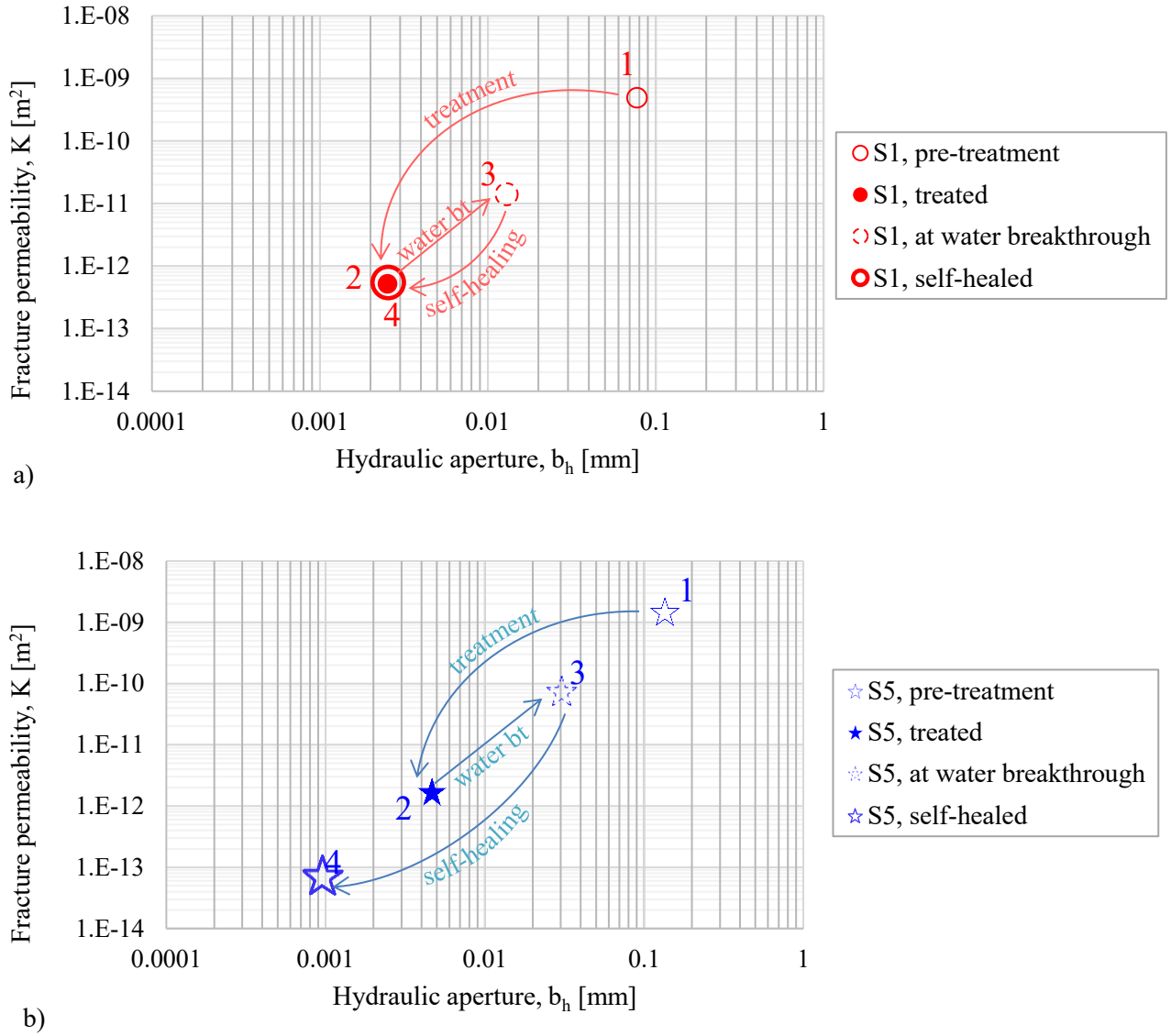

Figure 8. Evolution of fracture permeability as a function of hydraulic aperture before treatment (1), after treatment (2), at water breakthrough (3) and after self-healing (4) for a) core S1, and b) core S5

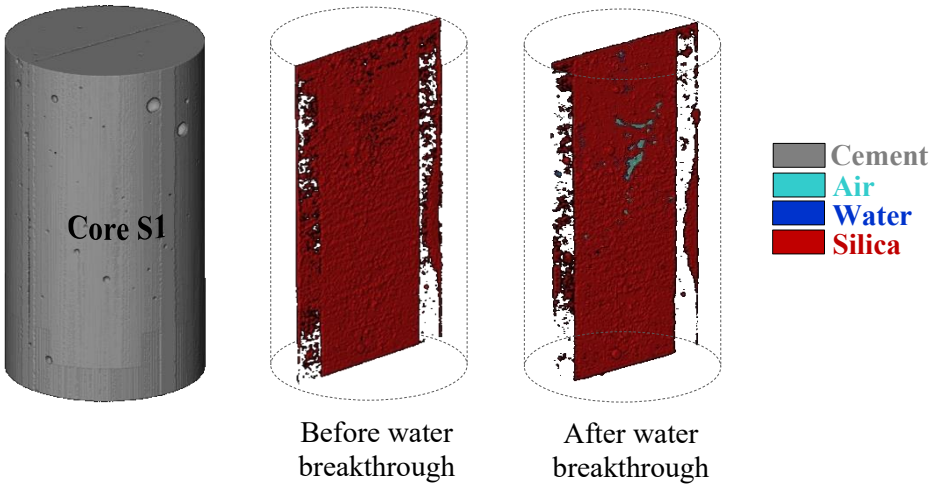

Figure 9. 3D volume rendering of 4 phases detected from x-ray tomographies – cement, air, water and silica –before and after water breakthrough (core S1).

4. CONCLUSIONS

This paper investigates the potential for using CS-based grout to provide long-term sealing of fluid migration pathways in oil & gas wells. An experimental investigation was carried out in this study to explore the pumpability of CS grout, and the effectiveness of CS grout treatment on fractured cement cores under pressure and temperature regimes typical of shallow North Sea wells (depths up to 1600 m). The experimental investigation showed that:

- CS grout prepared with no accelerator, or with NaCl accelerator at concentrations up to 0.5 M, would be suitable for pumping to depth up to ~1600 m, if a 2-hour pumping operation period is considered.

- Even in the absence of an accelerator, CS-based grout successfully reduced the permeability of fractured cement cores with constant fracture apertures of 0.2 mm and 0.5 mm, by 3 orders of magnitude. Fracture permeability values obtained after treatment were comparable to that of pure CS gel, suggesting the formation of a continuous gel matrix within the fracture. This evidence was

confirmed by X-CT microstructural analyses carried out on selected cores before and after treatment.

- Grout fracturing may occur depending on both the absolute pressure differential experienced downhole, and the exposure time to fluid flow through the gelled grout. For two of the six cores tested in this study, fracture permeability after fracturing at 1.45 MPa remained at least one order of magnitude lower than that of the untreated fractures.

- In the two cores which experienced fracturing, self-healing was shown to occur in the absence of continuous flow within 5 months. Fracture permeability after self-healing was comparable to, or even lower than that of treated cement before fracturing.

The substantial permeability reduction achieved in this study provides a proof of concept for the use of CS-based grout as a grouting material for sealing potential leakage pathways during plugging and abandonment operations. Colloidal silica injection could be achieved by pumping through the tubing, and could make use of existing perforations in casing, or be injected through new perforations to target sections with poor cement sheath integrity or where poor cement bond with the casing has been interpreted through the use of standard wellbore integrity logging techniques. In this study, we have demonstrated the potential of CS grout for repairing fine-aperture cracks within cement, which may exist within the sheath, at the cement/casing interface or within a cement wellbore barrier. CS grout could target cracks with apertures down to the size of hundreds of nanometres, where the use of conventional cementitious grouts would not be possible due to the relatively large size of cement particles. Additional experimental evidence would be required to investigate the performance and durability of the grout in the presence of relevant downhole fluids, including brines, hydrocarbons, CO_2-enriched brine, supercritical CO_2, and CH_4.

Acknowledgements

The authors gratefully acknowledge the financial support of the OGTC (Aberdeen, Scotland) under project WC-P-018, "Grouting of well leakage and migration pathways: Biogrouting and colloidal silica".

5. REFERENCES

Amiri, A., Øye, G. & Sjöblom, J., 2011. Temperature and pressure effects on stability and gelation properties of silica suspensions. *Colloids and Surfaces A: Physicochemical and Engineering Aspects,* Volume 378, pp. 14-21.

Bahadur, A. K., Holter, K. G. & Pengelly, A., 2007. Cost-effective pre-injection with rapid hardening microcement and colloidal silica for water ingress reduction and stabilisation of adverse conditions in a headrace tunnel. Dans: H. R. &. Z. Barták, éd. *Underground Space – the 4th Dimension of Metropolises.* London: Taylor & Francis Group, pp. 297-301.

Böttner, C. et al., 2020. Greenhouse gas emissions from marine decommissioned hydrocarbon wells: leakage detection, monitoring and mitigation strategies. *International Journal of Greenhouse Gas Control,* Volume 100.

Butrón, C., Axelsson, M. & Gustafson, G., 2009. Silica sol for rock grouting: Laboratory testing of strength, fracture behaviour and hydraulic conductivity. *Tunnelling and Underground Space Technology,* Volume 24, p. 603–607.

Butrón, C., Gustafson, G., Fransson, Å. & Funehag, J., 2010. Drip sealing of tunnels in hard rock: A new concept for the design and evaluation of permeation grouting. *Tunnelling and Underground Space Technology,* Volume 25, p. 114–121.

Celia, M. A. et al., 2005. Quantitative estimation of CO2 leakage from geological storage: Analytical models, numerical models, and data needs. *Greenhouse Gas Control Technologies 7 - Proceedings of the 7th International Conference on Greenhouse Gas Control Technologies 5– September 2004, Vancouver, Canada,* Volume I, pp. 663-671.

Gasda, S. E., Bachu, S. & Celia, M. A., 2004. Spatial characterization of the location of potentially leaky wells penetrating a deep saline aquifer in a mature sedimentary basin. *Environmental Geology,* Volume 46, pp. 707-720.

Hakem, N., Al Mahamid, I., Apps, J. & Moridis, G., 1997. *Sorption of Cesium and Strontium on Savannah River Soils Impregnated with Colloidal Silica.* Petersburg, s.n.

Hunt, J. D., Ezzedine, S. M., Bourcier, W. & Roberts, S., 2013. *KINETICS OF THE GELATION OF COLLOIDAL SILICA AT GEOTHERMAL CONDITIONS, AND IMPLICATIONS FOR RESERVOIR MODIFICATION AND MANAGEMENT.* Stanford, s.n.

Iler, R. K., 1979. *The Chemistry of Silica: Solubility, Polymerization, Colloid and Surface Properties, and Biochemistry.* s.l.:John Wiley & Sons.

Jurinak, J. J. & Summers, L. E., 1991. Oilfield Applications of Colloidal Silica Gel. *SPE Production Engineering,* Volume 406-412.

Kiran, R. et al., 2017. Identification and evaluation of well integrity and causes of failure of well integrity barriers (A review). *Journal of Natural Gas Science and Engineering,* Volume 45, pp. 511-526.

Manchester, K. et al., 2001. *Grout Selection and Characterization in Support of the Colloidal Silica Barrier Deployment at Brookhaven National Laboratory.* Orlando, s.n.

Moridis, G. J., Finsterle, S. & Heiser, J., 1999. Evaluation of alternative designs for an injectable subsurface barrier at the Brookhaven National Laboratory site, Long Island, New York. *Water Resources Research,* 35(10), pp. 2937-2953.

Moridis, G. et al., 1995. *A field test of permeation in heterogeneous soils using a new generation of barrier liquids. Committed To Results: Barriers for Long-Term Isolation..* s.l., s.n.

Nguyen, P., Guthrie, G. D. J. & Carey, W., 2020. Experimental validation of self-sealing in wellbore cement fractures exposed to high-pressure, CO2-saturated solutions. *International Journal of Greenhouse Gas Control,* Volume 100.

Oil & Gas UK, 2020. *Decommissioning Insight 2020,* s.l.: s.n.

Pedrotti, M., Wong, C., El Mountassir, G. & Lunn, R. J., 2017. An analytical model for the control of silica grout penetration in natural groundwater systems. *Tunnelling and Underground Space Technology,* Volume 70, pp. 105-113.

Persoff, P., Apps, J., Moridis, G. & Whang, J. M., 1999. Effect of dilution and contaminant on sand grouted with colloidal silica. *Jouranl of Geotechnical and Geoenvironmental Engineering,* 125(6), pp. 461-469.

Persoff, P. et al., 1995. *Injectable Barriers for Waste Isolation.* s.l., s.n.

Vrålstad, T. et al., 2019. Plug & abandonment of offshore wells: Ensuring long-term well integrity and cost-efficiency. *Journal of Petroleum Science and Engineering,* Volume 173, pp. 478-491.

Witherspoon, P. A., Wang, J. S. Y., Iwai, K. & Gale, J. E., 1980. Validity of Cubic Law for Fluid Flow in a Deformable Rock Fracture. *Water Resources Research,* 16(6), pp. 1016-1024.

Yates, P. C., 1990. *Kinetic of gel formation of colloidal silica sols. In: 200th National meeting: Abstract.* s.l., s.n.